PERGAMON

International Journal of Multiphase Flow 25 (1999) 857–874

International Journal of Multiphase Flow

www.elsevier.com/locate/ijmulflow

Investigation of two-phase flow regimes in tube bundles under cross-flow conditions

G.R. Noghrehkar[a], M. Kawaji[a,*], A.M.C. Chan[b]

[a]*Department of Chemical Engineering and Applied Chemistry, University of Toronto, Toronto, Ontario, Canada, M5S 3E5*

[b]*Ontario Hydro Technologies, Toronto, Canada*

Received 15 May 1998; received in revised form 6 November 1998

Abstract

Two-phase flow regimes in tube bundles have been determined in vertical upward cross-flow of air and water in horizontal tube bundles. Experiments were conducted using staggered and in-line tube bundles with a pitch-to-diameter ratio of 1.47, containing respectively 26 and 24 rows of five 12.7 mm O.D. tubes in each row. A resistivity void probe was used to measure the local void fraction and the probability density function (PDF) of local void fraction fluctuations was used in an objective statistical method to determine the two-phase flow regimes. For the in-line tube bundle, a bubbly flow regime occurred for $J_G < 0.4$–0.8 m/s and an intermittent flow regime for J_G between 0.4–1.0 m/s and 3.9 m/s at all liquid flow rates tested ($J_L < 1.0$ m/s). An annular flow regime occurred for $J_G > 3.9$ m/s at only low liquid flow rates ($J_L < 0.25$ m/s). Compared to the previous flow regime maps, the intermittent flow regime was found to persist up to much higher liquid flow rates, and this was attributed to the difference in the flow regime identification methods used. The limitation of the visual observation technique for flow regime identification in tube bundles became evident as significantly different amplitudes of void fluctuations were measured and different flow regimes were shown to exist near the shell wall and inside the tube bundle. For the staggered tube bundle, the results were similar except for bubbly-intermittent flow regime transition which occurred at higher gas flow rates compared to the in-line tube bundle, possibly due to more efficient break-up of large gas slugs.

* Corresponding author. Fax: + 1-416-9788605.
E-mail address: kawaji@ecf.utoronto.ca (M. Kawaji)

0301-9322/99/$ - see front matter
PII: S0301-9322(98)00075-5

1. Introduction

Two-phase cross flow occurs in various sizes and types of tube bundles in process heat exchangers, kettle reboilers and the U-bend region of steam generators used in nuclear power plants. It has been estimated that nearly half of all process heat exchangers operate in two-phase flow, however, our understanding of two-phase cross flow in tube bundles is far from satisfactory, in comparison with that in circular tubes.

Efficient designs of shell-and-tube heat exchangers often require high fluid velocities on the shell side while an optimum design would necessitate as much reduction in the structural support as possible. However, the high fluid velocities and reduced structural support can lead to excessive flow-induced vibrations of tubes in these components, which could cause tube failures. The nature of two-phase flow regimes inside tube bundles is an important consideration in predicting the two-phase flow-induced vibration phenomena (Pettigrew and Taylor, 1994). Although many previous studies have addressed two-phase flow regimes inside tubes, fewer experimental studies have dealt with flow regimes for upward two-phase flow across horizontal tube bundles. This is not surprising since the measurements required for flow regime identification inside the tube bundle are more difficult to make, and consequently the experiments have been restricted to visual observations of two-phase flow regimes from outside the tube bundle.

Grant and Murray (1972) used a segmentally baffled transparent model heat-exchanger of a rectangular cross section containing 39 tubes of 19 mm O.D., arranged in an equilateral triangle layout with a pitch-to-diameter ratio (p/d) equal to 1.25. Their experiments were carried out in vertical cross-flow of air and water, and the two-phase flow regimes were determined by visual observations through transparent tube end plates. They identified bubbly, intermittent and dispersed (spray) flow regimes and proposed a flow regime map based on dimensionless superficial gas and liquid velocities.

Kondo and Nakajima (1980) performed experiments on vertical air–water cross-flow in a staggered tube bundle and identified flow regimes by visual observation. They classified the observed flow regimes into bubbly, slug, froth and spray flows; however, their experiments were limited to very small liquid flow rates ($J_L \leq 0.005$ m/s). Pettigrew et al. (1988) conducted two-phase cross-flow studies in connection with flow-induced tube vibration phenomena, and reported a limited amount of flow regime data obtained based on visual observations of flows from outside the tube bundle.

Hahne et al. (1990) used a fiber optics probe to measure local void fraction using refrigerant R11 under pool boiling conditions in in-line and staggered tube bundles consisting of 18 low-finned tubes with $p/d = 1.3$ and 1.15. Probability density histograms of local void fractions and their higher moments were used to identify the flow regimes inside the tube bundle. Only a bubbly flow regime was detected and no slug or annular flow regimes were observed within the tube bundle. The detection of only the bubbly flow regime could have been due to a limited range of flow conditions obtainable under the pool boiling conditions, and a combination of narrow gaps and presence of fins which may have broken up large vapor slugs into smaller bubbles.

Ulbrich and Mewes (1994) have recently studied vertical two-phase flow of air and water across a horizontal tube bundle with 10 rows of five tubes (per row) with 20 mm O.D. and

200 mm length. The tubes were arranged in a square in-line layout with a p/d ratio of 1.5 in a rectangular shell. Flow regimes were determined by visual observation using still and video photography over superficial liquid and gas velocities of 0.001–0.65 m/s and 0.047–9.3 m/s, respectively. Time traces of pressure drop measured between the second and ninth rows were also used to aid in their flow regime identification.

Ueno et al. (1995) employed double-sensor probes to measure the local void fraction, interfacial area concentration, bubble frequency and interfacial velocity for vertical upward flow of an air–water mixture across a 2×20 in-line tube bundle with $p/d = 1.42$. The flow passage was a gap between two half-rods attached to opposite walls. Void fraction profiles in axial and transverse directions were obtained. Slug flow was identified by large size bubbles, which had crowds of small bubbles in their tail, flowing mainly in the gap region. They also noted that gas slugs do not have a bullet shape, which is often observed in circular pipes.

The characteristics of the two-phase cross flow in tube bundles have also been experimentally investigated by others, such as Lian et al. (1992, 1997), Schrage et al. (1988), Dowlati et al. (1990, 1992a, 1992b, 1996), Boivin et al. (1987), Haquet and Gouirand (1995) and Remy (1982), among others; however, most of these studies concentrated on void fraction and pressure drop measurements, or two-phase cross-flow induced vibration of tubes in horizontal tube bundles. They provide little information on two-phase flow regimes in tube bundles. Dowlati (1992) noted that some two-phase flow regimes determined by visual observation from outside the bundle occurred under significantly different conditions from those observed in a circular tube. In particular, bubbly flow appeared to persist up to a much higher void fraction of about 60% compared to about 30% in tubes. Since visual observations of two-phase flow from outside the tube bundle may only disclose the nature of flow near the wall, the actual flow regime inside the bundle may not be the same as that observed from outside.

In order to identify two-phase flow regimes in an objective manner, Jones and Zuber (1975) were among the first to use a non-visual technique, based on X-ray void fraction measurements. They measured void fluctuations in air–water upward flow in a narrow rectangular channel (5×64 mm). The probability density function (PDF) of void fluctuations was successfully used to identify bubbly, slug and annular flow regimes. The PDF distributions showed a single peak at low void fraction for bubbly flow, a single peak at high void fraction for annular flow, and two peaks for slug or intermittent flow, one characteristic of bubbly flow and the other characteristic of annular flow. The PDFs of other flow parameters such as pressure and differential pressure (Matsui, 1984) and void fraction measured by electrical resistivity probes (Ali et al., 1993) have been used as objective indicators of two-phase flow regimes in circular and narrow channels.

The objectives of this work are to determine the two-phase flow regimes inside in-line and staggered tube bundles using probability density functions of local, instantaneous void fractions measured inside the bundles and to examine the effect of tube bundle geometry on two-phase flow regime maps. In order to achieve these objectives, an air–water two-phase flow loop was used along with a resistivity void probe inserted deep into the bundles, and two-phase flow regime maps were developed for both in-line and staggered tube bundles.

2. Experimental facility and procedure

2.1. Test loop

An air–water two-phase flow loop consisted of a reservoir tank, air–water separator tank, centrifugal pump, flow control valves, flow meters, test section, air supply system and related piping, as shown in Fig. 1. The loop was designed to accept tube bundle test sections up to 0.6 m in height with a rectangular cross-section of 200 × 110 mm. Water stored in the reservoir tank was pumped using a centrifugal pump with a capacity of 0.02 m^3/s and powered by a 10 kW motor, through one of two orifice flow meters with measurement ranges of 0–6 and 6–15 l/s, into a liquid inlet nozzle located at the bottom of the test section. Air from the building supply at 200 kPa was filtered and its pressure reduced through a regulator and the air flow rate was measured using a bank of rotameters. Air was then injected into the entrance of the test section through both a 38 mm O.D. porous tube that extended across the test section normal to the tube axis and a 25.4 mm O.D. porous tube that was placed along the test section axis.

The two-phase mixture traveled up through a rectangular test section containing either an in-line or staggered tube bundle and exited through a nozzle into an open-top gas–liquid separator tank as shown in Fig. 2. Flow straighteners in the form of parallel plates (300 mm long) were located 50 mm above the air injection nozzles and 80 mm below the tube bundle. Flow visualization revealed that the air–water flow was well mixed before reaching the first row of the tube bundle. The top of the tube bundle was located approximately 300 mm below

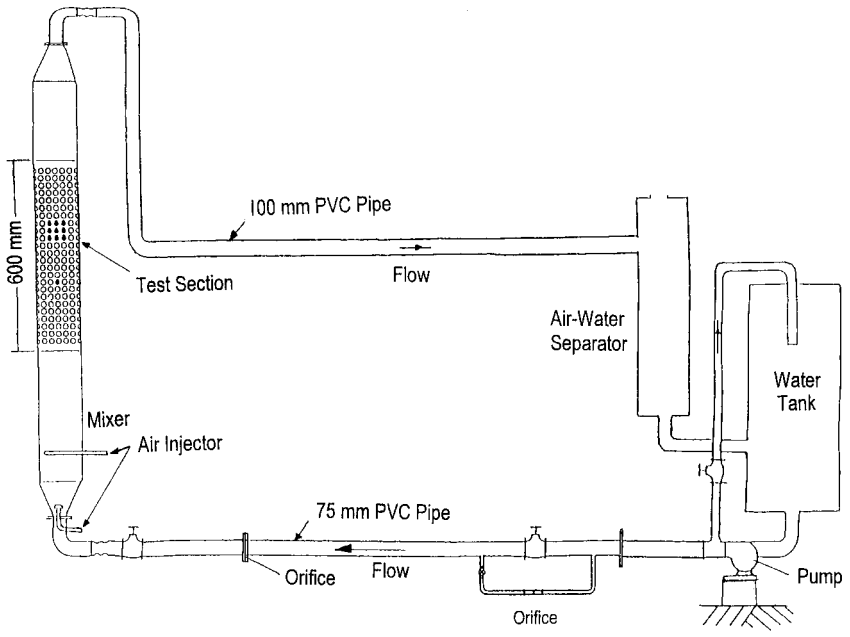

Fig. 1. Air–water two-phase flow loop.

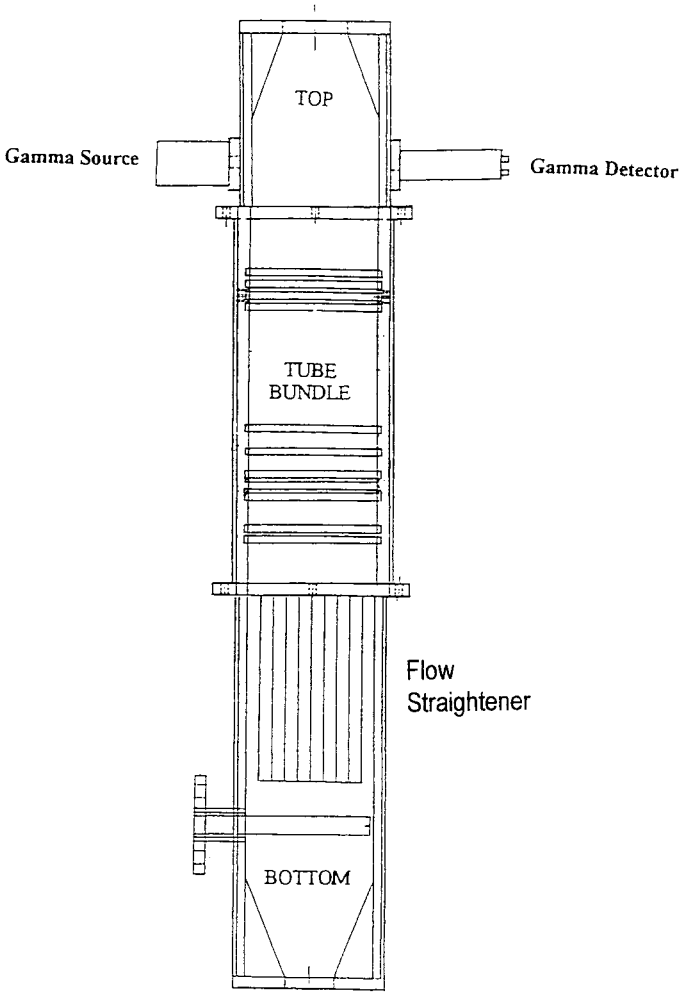

Fig. 2. Schematic of cross flow test section.

the exit nozzle in the upper plenum and diffuser plates were placed below the exit nozzle to obtain smooth flow out of the test section.

Two different tube bundles were constructed for two-phase cross-flow tests. One was an in-line tube bundle with 24 rows of five full tubes and two half tubes, and the second was a staggered tube bundle with 26 rows, as shown schematically in Fig. 3. The tubes in both bundles were 200 mm long and 12.7 mm O.D. There were five tubes per row arranged with a pitch-to-diameter ratio, $p/d = 1.47$. Half tubes were installed on the test section side walls to minimize bypass leakage and to reduce the wall effects. The tubes and the shell were all made from transparent acrylic, which allowed for flow visualization.

The experiments were performed at a test section pressure slightly above atmospheric and at 22°C by varying the superficial liquid velocity, J_L, from 0.05 to 1.0 m/s (or mass flux from 50 to 1000 kg/m^{2}s) and superficial gas velocity, J_G, from 0.02 to 3.9 m/s (or the homogeneous

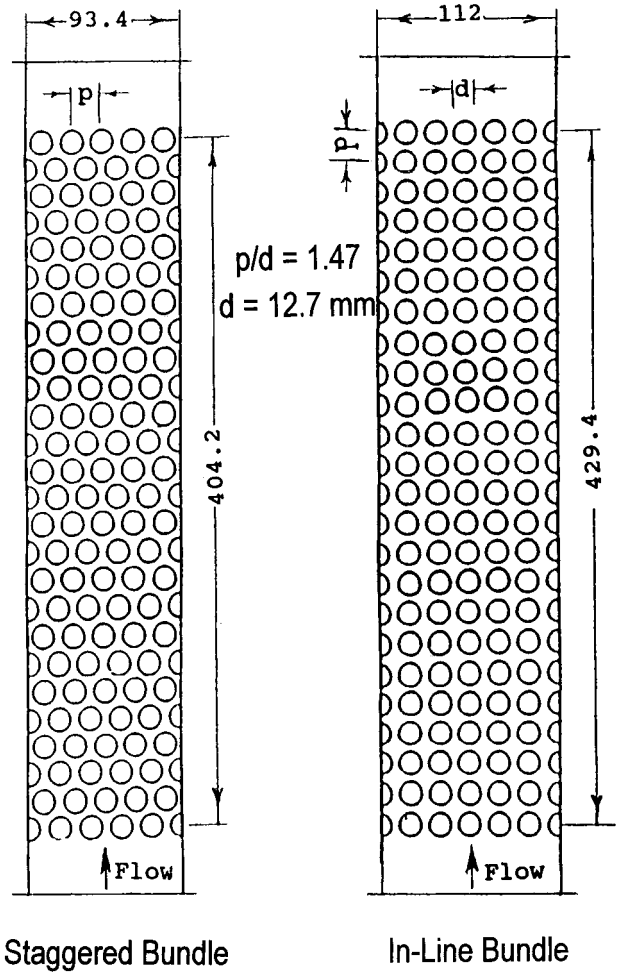

Fig. 3. In-line and staggered tube bundles.

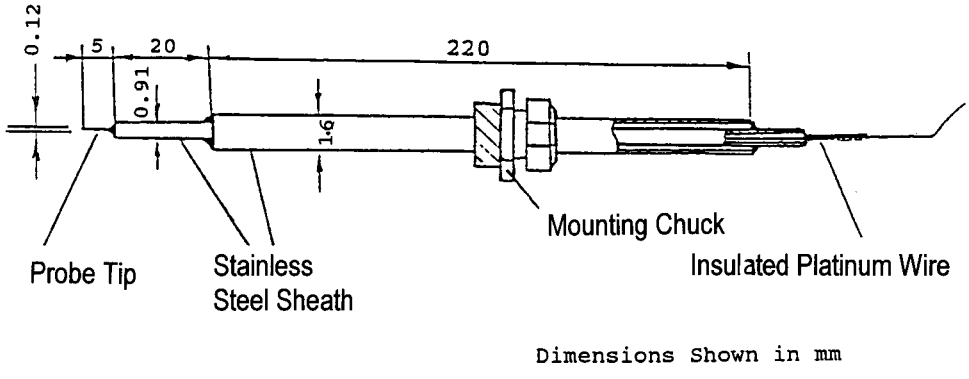

Fig. 4. Electrical resistivity void probe.

void fraction from 0 to 98%). A personal computer based data acquisition system with a Keithley Metrabyte Model DAS-16 high speed A/D data acquisition board and Viewdac sofware was used to record the flow rate data and the void signal from a resistivity void probe described below.

2.2. Resistivity void probe

An electrical resistivity probe was fabricated and mounted inside the in-line and staggered tube bundles to measure the local instantaneous void fractions. The resistivity probe, schematically shown in Fig. 4, was made of a Teflon-coated platinum wire of 0.12 mm O.D. inserted into a 0.5 mm I.D., 0.91 mm O.D. stainless steel tube. The probe tip was covered with epoxy cement except at the tip, so that the exposed platinum wire tip acted as the first electrode and the stainless steel sheath as the second electrode. The electrodes were electrically connected in series with a resistor, to a DC voltage source. The probe was installed in the tube gap at the fifth row of the in-line tube bundle and the sixth row of the staggered tube bundle, and the probe tip was placed as close to the central location of the bundle as possible.

The operation of the resistivity probe is based on a difference in electrical resistivity between the liquid and gas phases. An electric potential (5 V DC) was applied between the platinum wire and the stainless steel sheath, and the change in electrical conductivity of the fluid surrounding the probe tip was measured. The output signal of the resistivity probe was sampled at a frequency of 5 kHz, and a threshold voltage was used to compute the void fraction. The ratio of the number of samples in which the output voltage was below the threshold level to the total number of samples in a short interval of time (10 ms) gave the local, instantaneous void fraction at the probe tip.

In order to establish the threshold level, the void probe was calibrated against a gamma densitometer, in which gamma ray attenuation is used to measure chordal-average void fraction over the gamma beam path. A single-beam gamma densitometer was used with a well-collimated rectangular beam, 50 mm wide by 10 mm high, from a 2 mCi cesium-137 gamma source emitting a 662 keV gamma ray. The transmitted gamma ray intensity was detected by a thallium activated sodium iodide, NaI(Tl), scintillation detector and then processed using a standard pulse-counting system. The details of the design and operation of the gamma densitometer can be found in Chan and Banerjee (1981). The gamma densitometer was installed in the upper plenum above the tube bundle as shown in Fig. 2, along with the resistivity void probe. Void fraction measurements were then performed over a wide range of liquid and gas flow rates, and the void probe's threshold voltage level was chosen so as to match the time-averaged void fractions determined from the void probe signal with those measured by the gamma densitometer. The relative uniformity of void fraction in the upper plenum was also checked by making the local void fraction measurements with the void probe at three locations along the gamma beam path.

The details of the experimental apparatus, instrumentation, calibration and experimental procedure can be found in Noghrehkar (1996).

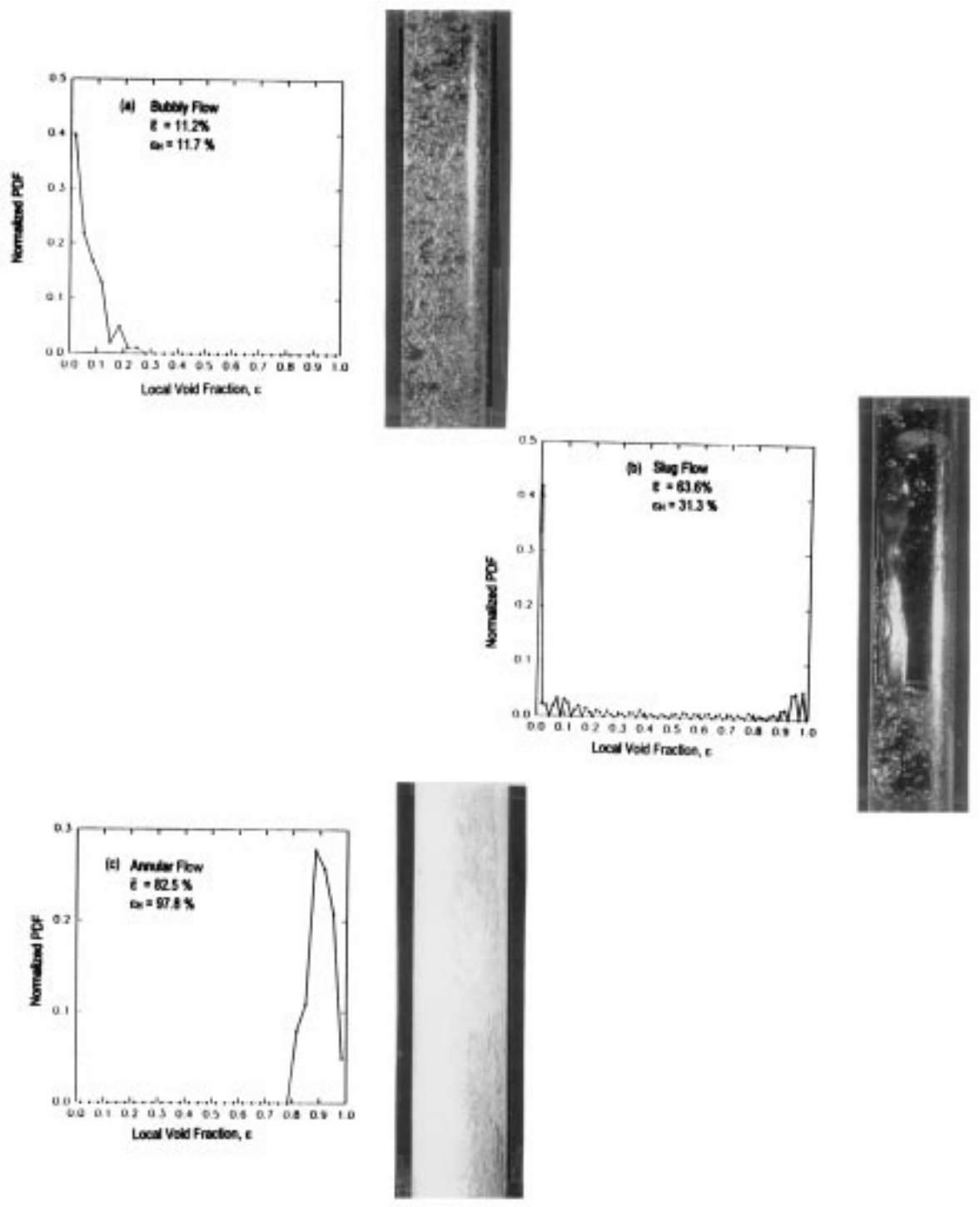

Fig. 5. Probability density functions of void fluctuations for (a) bubbly flow, (b) slug flow, and (c) annular flow obtained in vertical tube.

2.3. Probability density function (PDF) of void fraction and flow regime identification

The instantaneous local void fraction data were used to calculate the PDF of local void fraction. If $P(\varepsilon)$ is the probability that the void fraction, ε, is less than some specific value, then $dP(\varepsilon)/d\varepsilon = p(\varepsilon)$ represents the probability per unit void fraction that the void fraction lies between the values of ε and $\varepsilon + d\varepsilon$. If the void fraction and the time scale are divided into equal increments of $\Delta\varepsilon_i$ and Δt_i, respectively, and during the total time interval T, the void fraction is in $\Delta\varepsilon_i$ a total of n_i times, and N is the total number of void fraction data recorded in interval T, then:

$$\frac{n_i/N}{\Delta\varepsilon_i} = \frac{1}{\Delta\varepsilon_i}\sum_{j=1}^{n_i}\frac{\Delta t_j}{T} \tag{1}$$

The ratio, $\Delta t_j/T$, is the probability that the void fraction lies within the given interval $\Delta\varepsilon_i$. Then the probability density function can be given by:

$$\lim_{\Delta\varepsilon_i\to 0}\frac{1}{T\Delta\varepsilon_i}\sum_{j=1}^{n_i}\Delta t_j \tag{2}$$

If a small enough value is chosen for Δt_i, the PDF may be estimated using the left or right hand side of Eq. (1). In the present work, the PDF of the local instantaneous void fraction was computed using

$$PDF = \frac{n_i/N}{\Delta\varepsilon_i} \tag{3}$$

and $\Delta\varepsilon_i = 0.02$. Ali et al. (1993) had used the same flow regime identification technique successfully with $\Delta\varepsilon = 0.025$, and the present value was again small enough to yield the PDF profiles adequate for flow regime identification.

To verify the present flow regime identification method based on PDFs of void fraction, separate experiments were conducted in a vertical transparent tube with 35 mm I.D. installed in another air–water flow loop. The void probe was inserted and placed at the tube axis and the PDFs of void fraction were obtained and compared to the visually observed flow regimes. The flow regimes deduced from PDFs based on Jones and Zuber's (1975) criteria agreed well with those observed visually, and the examples of the PDF distributions and the photographs of the flow regimes are shown in Fig. 5. The PDF data showed (a) a single peak at a low void fraction for bubbly flow, (b) two peaks, one each at low and high local void fractions, for slug or churn-turbulent flow (collectively called intermittent flow), and (c) a single peak at a high local void fraction for annular or annular-mist flow.

Another parameter which could be readily derived from the void fraction data and examined during flow regime identification is the root-mean square (rms) amplitude of the local void fraction fluctuations. This can be calculated as,

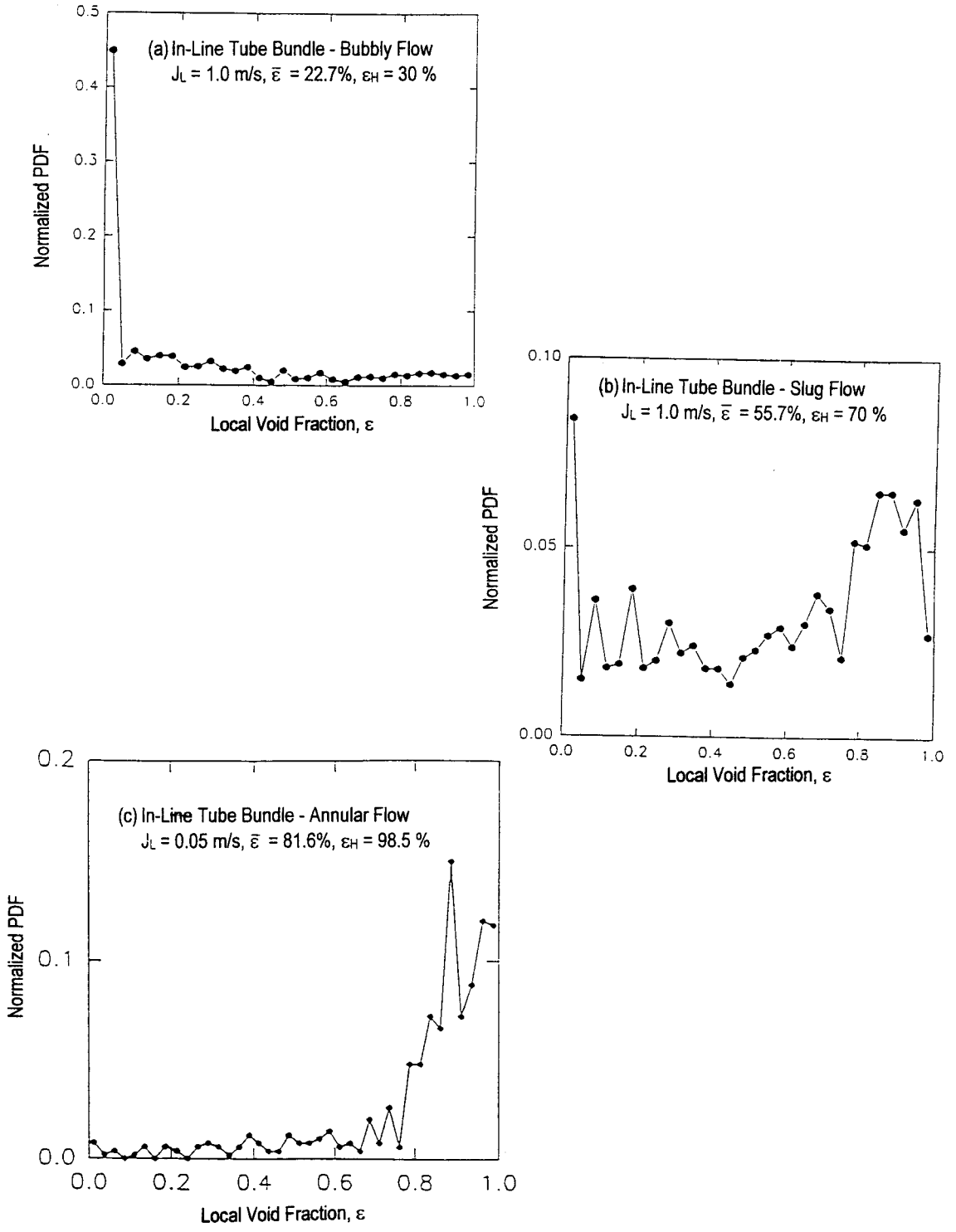

Fig. 6. Probability density functions of void fluctuations for (a) bubbly flow, (b) slug flow, and (c) annular flow obtained in an in-line tube bundle.

$$\varepsilon_{\mathrm{rms}} = \sqrt{\frac{\sum_{i=1}^{N}(\varepsilon_i - \bar{\varepsilon})^2}{N}} \tag{4}$$

where ε_i is the instantaneous local void fraction, $\bar{\varepsilon}$ is the time-averaged local void fraction over the total sampling time, T.

3. Results and discussion

3.1. Flow regime maps

The PDF technique was applied to the objective determination of two-phase flow regimes in both in-line and staggered tube bundles. Typical PDFs of local void fractions measured well inside the tube bundles are shown in Fig. 6. From the PDF data, three types of flow regimes commonly found in pipes can again be objectively determined; bubbly flow, intermittent flow and annular flow.

Two-phase flow regime maps were then constructed using the PDF technique for both in-line and staggered tube bundles as shown in Figs. 7 and 8, respectively. For the in-line tube bundle (Fig. 7), the bubbly flow regime was observed at low gas flow rates ($J_G < 0.4$–1.0 m/s) and the intermittent flow regime occurred for intermediate superficial gas velocities (0.4 m/s $< J_G <$ 3.9 m/s), at all liquid flow rates. Annular flow was observed at J_G greater than 3.9 m/s only for

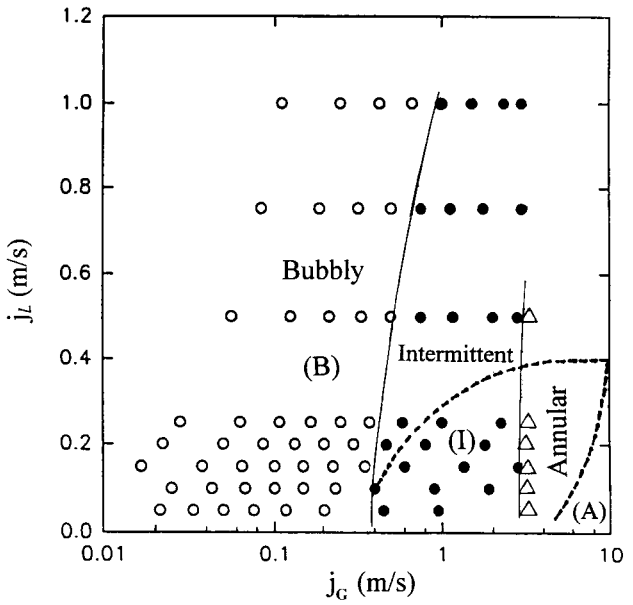

Fig. 7. Flow regime map for in-line tube bundle and comparison with the map proposed by Ulbrich and Mewes (1994).

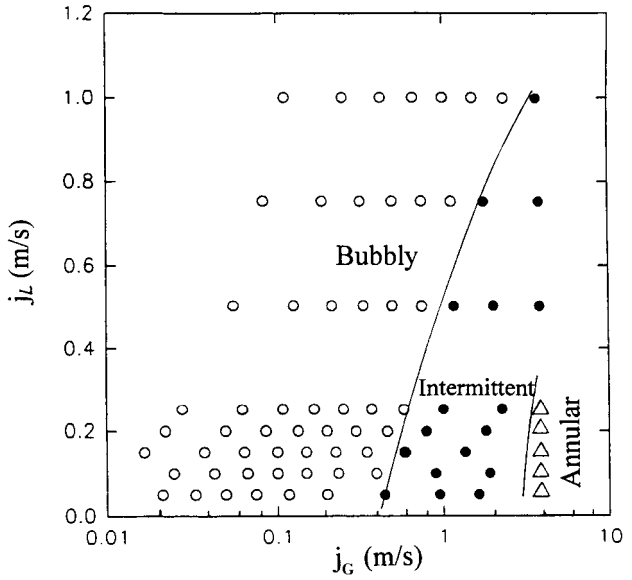

Fig. 8. Flow regime map for staggered tube bundle.

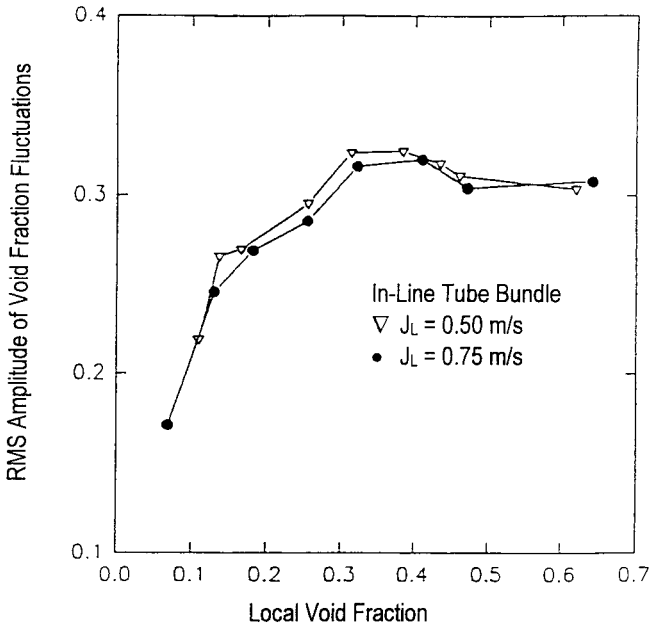

Fig. 9. Variation of rms amplitude of local void fluctuations with time-averaged local void fraction for in-line tube bundle.

low liquid flow rates (J_L < 0.5 m/s). The superficial gas velocity at which bubbly to intermittent flow regime transition occurred increased from 0.4 to 1.0 m/s for increasing superficial liquid velocity, J_L, from 0.05 to 1.0 m/s. On the other hand, the intermittent to annular flow regime transition occurred at a constant superficial gas velocity of about 3.9 m/s, independent of liquid flow rate, for J_L < 0.5 m/s. At higher liquid flow rates, the maximum gas flow rate that could be delivered in the present work was insufficient to cause transition from intermittent to annular flow.

For the staggered tube bundle (Fig. 8), the flow regime map obtained was similar to that described above for the in-line tube bundle. The bubbly flow regime was again observed at low superficial gas velocities (J_G < 0.45–2.0 m/s) for J_L between 0.05 and 1.0 m/s, and intermittent flow occurred at intermediate gas flow rates (J_G < 3.9 m/s). Annular flow was observed at J_G > 3.9 m/s at low liquid flow rates, J_L < 0.25 m/s.

To check the sensitivity of the PDFs of void fluctuations and the flow regime results to the void measurement location, the void probe was moved to the thirteenth row from the fifth row of the in-line tube bundle, and the local void fraction measurements were repeated under the same flow conditions. There were no notable differences between the PDFs obtained at the two different locations under the same flow conditions. Thus, the flow regime maps presented in Figs. 7 and 8 can be considered to be insensitive to the void probe location and to represent the flow regimes occurring in the entire bundle.

To further support the PDF results, the rms amplitudes of local void fraction fluctuations were determined, and the data for $J_L = 0.5$ and 1.0 m/s (mass flux of 500 and 750 kg/m^{2}s) are

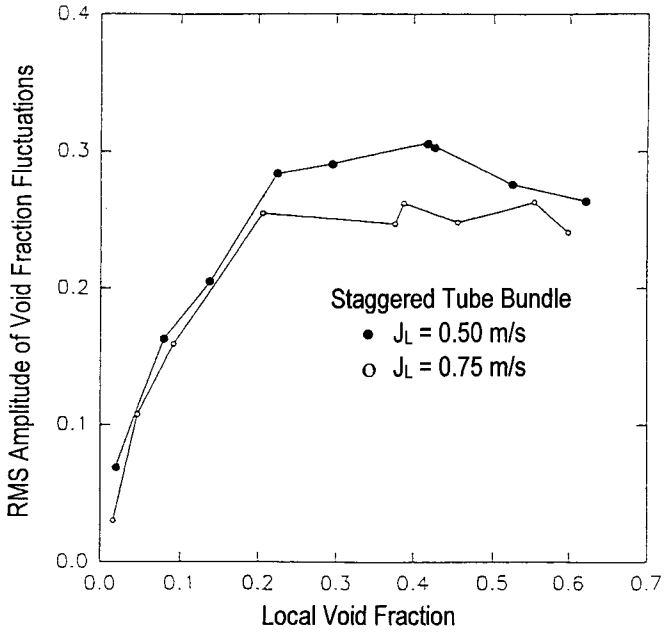

Fig. 10. Variation of rms amplitude of local void fluctuations with time-averaged local void fraction for staggered tube bundle.

plotted against the time-averaged local void fraction in Figs. 9 and 10 for the in-line and staggered tube bundles, respectively. These figures show that at those liquid flow rates where intermittent flow regime occurs in both bundles, the rms amplitude of local void fraction fluctuations increases with increasing void fraction up to $\varepsilon = 30\%$ in bubbly flow regime, reaches a peak at about $\varepsilon = 40\%$ and then decreases slightly at higher void fractions in the intermittent flow regime.

Since the void fluctuation amplitudes are not significantly different between the two bundles for the intermittent flow regime, the effect of the void probe location with respect to the tubes can be considered to be small. In the in-line bundle, the probe was placed in one of the tube gaps which formed a straight, upward flow passage. In the staggered bundle, the void probe was also placed in the tube gap but directly behind another tube in the preceding row. Although the staggered bundle presented a more tortuous flow passage for the two-phase mixture than the in-line tube bundle, similar amplitudes of void fluctuations detected in the two bundles indicate similar sizes of gas slugs flowing inside the two bundles.

3.2. Comparison with previous flow regime maps

The flow regime map obtained for the present in-line tube bundle is next compared with that obtained by Ulbrich and Mewes (1994) for a smaller in-line tube bundle (10 rows × five tubes/row) with $p/d = 1.5$ as shown by dashed lines in Fig. 7. From this figure, it can be noted that, although the bubbly flow regime was detected over similar ranges of gas and liquid flow rates, the intermittent flow regime was not detected in their tests for $J_L > 0.4$ m/s at any gas flow rate up to $J_G = 9.3$ m/s. Similar results were also reported in the flow regime maps of Grant and

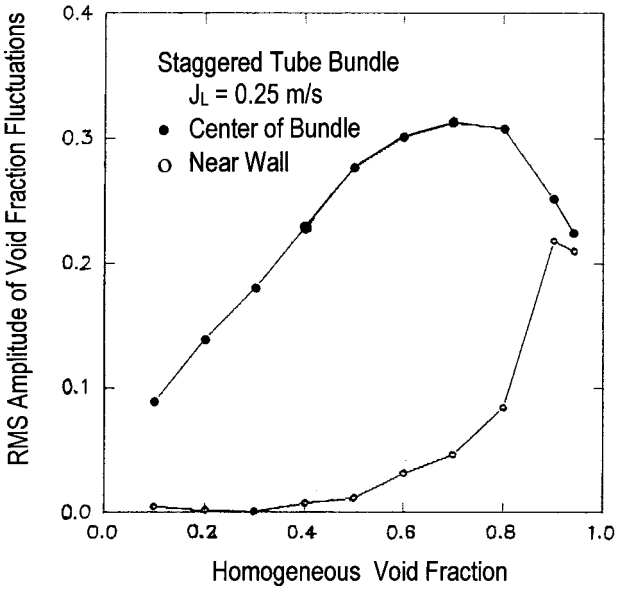

Fig. 11. Comparison of void fluctuation amplitude between inside-bundle and near-wall regions in staggered bundle ($J_L = 0.25$ m/s).

Murray (1972) and Grant and Chisholm (1979), who also used visual observation for flow regime identification. The absence of intermittent flow from the flow regime maps of Ulbrich and Mewes (1994) and Grant and Murray (1972) for $J_L > 0.4$ m/s at all superficial gas flow rates below 10 m/s is significantly different from the present results, and can be attributed to the use of different flow regime identification techniques.

Although Ulbrich and Mewes (1994) measured and analyzed pressure drop fluctuations across the bundle to aid in flow regime identification unlike in Grant and Murray's (1972) experiments, both relied on visual observations and photographic or video recordings of flow regimes from outside the bundle. The visual observation technique has been used successfully for two-phase flow regime identification in tubes; however, its application to a tube bundle may not be always reliable, since the flow regime that can be visually observed is only the flow near the shell wall and not necessarily the flow regime existing well inside the tube bundle.

To verify this point, the local void fraction was measured at a location 5 mm away from the shell wall and the rms amplitude of local void fraction fluctuations was compared to the data obtained well inside the staggered tube bundle for $J_L = 0.25$ and 0.5 m/s, as shown in Figs. 11 and 12, respectively. Under the flow conditions tested, an intermittent flow regime existed within the staggered bundle over a wide range of homogeneous void fraction, but the void fluctuation amplitude remained very low near the wall, which is representative of bubbly flow. Thus, even under the same flow condition, the flow regimes that exist near the shell wall and well inside the bundle can be quite different. Visual observations of the flow from outside the bundle indicated the passage of numerous small bubbles under the flow conditions tested, which would be interpreted as bubbly flow, but the flow regime inside the bundle was

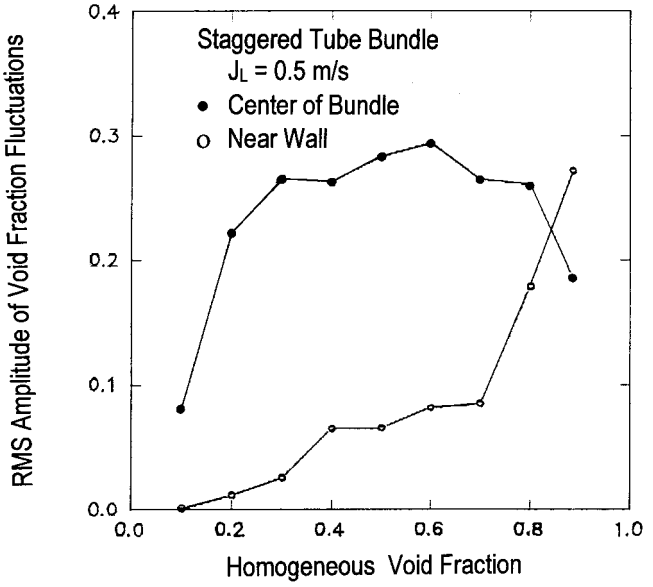

Fig. 12. Comparison of void fluctuation amplitude between inside-bundle and near-wall regions in staggered bundle ($J_L = 0.5$ m/s).

intermittent flow. These results clearly show that the visual observation technique applied to tube bundles even with the use of a still or video camera, may not always reveal the actual flow regime inside the tube bundle.

3.3. Effect of bundle geometry on two-phase flow regime maps

Flow regime maps for the in-line and staggered tube bundles were shown in Figs. 7 and 8. It can be seen from these figures that the effect of bundle geometry on the two-phase flow regime at low superficial liquid velocities is not significant. As the superficial liquid velocity increases, the transition from the bubbly to intermittent flow regime occurs at higher gas velocities or higher void fractions for the staggered tube bundle compared to the in-line tube bundle. This can be related to the smaller void fluctuation amplitudes in the staggered tube bundle than in the in-line tube bundle as evident from a comparison of Figs. 9 and 10. The rms amplitude of local void fluctuations is clearly lower for the staggered tube bundle than the in-line bundle and the effect of mass velocity on the amplitude of void fluctuations, as shown in Fig. 10, is also stronger for the staggered tube bundle in the intermittent flow regime.

From these results, the staggered tube bundle geometry is believed to be able to break up the gas phase into smaller bubbles more effectively, thereby reducing the amplitude of void fluctuations in the intermittent flow regime. Therefore, for the same flow conditions, the average gas bubble size and as a result the void fluctuation amplitude in staggered tube bundles is expected to be smaller than those in in-line tube bundles. This has important implications for damping of two-phase cross flow-induced vibration of tubes in tube bundles as recently discussed by Lian et al. (1997). They related tube damping phenomena to void fraction fluctuations, and showed similar dependence of tube damping ratio and void fluctuation amplitude on homogeneous void fraction.

4. Conclusions

The two-phase flow regimes in both in-line and staggered tube bundles have been experimentally investigated by measuring the local, instantaneous void fraction inside the tube bundles using a resistivity void probe and examining the void fraction fluctuations under vertical upward cross-flow conditions. The experimental results of this study can be summarized as follows:

1. The probability density function (PDF) of local void fraction has been successfully used in an objective manner to identify the two-phase flow regimes and construct flow regime maps for both in-line and staggered tube bundles. The flow regimes identified in these bundles were similar to those occurring in circular tubes and include bubbly, intermittent and annular flows.
2. There was a significant difference between the present flow regime map for an in-line tube bundle and those proposed previously by Ulbrich and Mewes (1994) and Grant and Murray (1972) concerning the occurrence of the intermittent flow regime at superficial liquid velocities greater than 0.4 m/s. This difference was attributed to the use of non-visual flow

regime identification method used in the present work and visual observation technique used in the previous experiments. The void fraction fluctuation amplitudes obtained well inside the bundle and close to the shell wall at two different liquid flow rates, indicated bubbly flow existing near the wall and intermittent flow inside the bundle under the same flow conditions. From this, it became clear that visual observations from outside the tube bundle may not always reveal the actual flow regime existing inside the bundle under certain flow conditions.

3. As the void fraction increases at a given superficial liquid velocity, a bubbly flow regime can exist over a wider range of superficial gas velocities in a staggered tube bundle than in an in-line tube bundle. This is attributed to the more efficient break-up of large gas slugs into smaller sizes in the staggered tube bundle that delays transition from bubbly to intermittent flow regime until a greater gas flow rate or larger void fraction is reached.

References

Ali, I.M., Kawaji, M., Sadatomi, M., 1993. Adiabatic two-phase flow in narrow channels between two flat plates. Can. J. Chem. Engng 71, 657–666.

Boivin, J.Y., Bussy, B., Pierotti, G., 1987. P.W.R. steam generators: a set of experimental programs for three dimensional code validation. In: Proceedings of ASME Winter Annual Meeting, Boston, MA, 13–18 December, pp. 1–6.

Chan, A.M.C., Banerjee, S., 1981. Design aspects of gamma densitometers for void fraction measurements in small scale two-phase flows. Nucl. Instrum. Meth. 190, 135–148.

Dowlati, R., 1992. Hydrodynamics of two-phase cross-flow and boiling heat transfer in horizontal tube bundles. Ph.D. Thesis, Department of Chemical Engineering and Applied Chemistry, University of Toronto.

Dowlati, R., Kawaji, M., Chan, A.M.C., 1990. Pitch-to-diameter effect on two-phase flow across an in-line tube bundle. AIChE J. 36, 765–772.

Dowlati, R., Kawaji, M., Chisholm, D., Chan, A.M.C., 1992a. Void fraction prediction in two-phase flow across a tube bundle. AIChE J. 38, 619–622.

Dowlati, R., Chan, A.M.C., Kawaji, M., 1992b. Hydrodynamics of two-phase flow across a horizontal in-line and staggered rod bundle. ASME J. Fluids Engng 114, 450–456.

Dowlati, R., Kawaji, M., Chan, A.M.C., 1996. Two-phase crossflow and boiling heat transfer in horizontal tube bundles. ASME J. Heat Transfer 118, 124–131.

Grant, I.D.R., Chisholm, D., 1979. Two-phase flow on the shell-side of a segmentally baffled shell-and-tube heat exchanger. ASME J. Heat Transfer 101, 38–42.

Grant, I.D.R., Murray, I., 1972. Pressure drop on the shell side of a segmentally baffled shell-and tube heat exchanger with vertical two-phase flow. Report NEL-500, National Engineering Laboratory.

Hahne, E., Spindler, K., Chen, Q., Windisch, R., 1990. Local void fraction measurements in finned tube bundles. In: Proceedings of the Ninth International Conference on Heat Transfer, Jerusalem, Israel, vol. 6, pp. 41–45.

Haquet, J.F., Gouirand, J.M., 1995. Local two-phase flow measurements in a cross-flow steam-generator tube bundle geometry: the Minnie II XF program. In: Proceedings of the 2nd International Conference on Multiphase Flow, Kyoto, Japan, 3–7 April, pp. 17–22.

Jones Jr, O.C., Zuber, N., 1975. The interrelation between void fraction fluctuations and flow patterns in two-phase flow. Int. J. Multiphase Flow 2, 273–306.

Kondo, M., Nakajima, K., 1980. Experimental investigation of air–water two phase upflow across horizontal tube bundles, Part I: flow pattern and void fraction. Bull. JSME 23 (177), 385–393.

Lian, H.Y., Chan, A.M.C., Kawaji, M., 1992. Effects of void fraction on vibration of tubes in tube bundles under

two-phase cross flow. In: Proceedings of 3rd International Symposium on Flow-Induced Vibration and Noise, vol. 1. ASME, New York, pp. 109–118.

Lian, H.Y., Noghrehkar, G., Chan, A.M.C., Kawaji, M., 1997. Effect of void fraction on vibration of tube bundles in two-phase cross flow. ASME J. Acoust. Vibr. 119, 457–463.

Matsui, G., 1984. Identification of flow regimes in vertical gas–liquid two-phase flow using differential pressure fluctuations. Int. J. Multiphase Flow 10, 711–720.

Noghrehkar, R., 1996. Investigation of local two-phase flow parameters in cross flow-induced vibration of tubes in tube bundles. Ph.D. Thesis, Department of Chemical Engineering and Applied Chemistry, University of Toronto.

Pettigrew, M.J., Taylor, C.E., 1994. Two-phase flow-induced vibration: an overview. ASME J. Pressure Vessel Technol. 166, 233–253.

Pettigrew, M.J., Taylor, C.E., Kim, B.S., 1988. Vibration of tube bundles in two-phase cross-flow—Part 1: hydrodynamic mass and damping. ASME J. Pressure Vessel Technol. 111, 446–477.

Remy, R.M., 1982. Flow induced vibration of tube bundles in two-phase cross-flow. In: Proceedings of the 3rd International Conference on Vibration in Nuclear Plants, Keswick, UK, vol. 1, pp. 135–160.

Schrage, D.S., Hsu, J.T., Jensen, M.K., 1988. Two-phase pressure drop in vertical cross flow across a horizontal tube bundle. AIChE J. 34, 107–115.

Ueno, T., Leung, W.H., Ishii, M., 1995. Local measurement in two-phase flow across a horizontal tube bundle. In: Proceedings of the 2nd International Conference on Multiphase Flow, Kyoto, Japan, 3–7 April, pp. 89–95.

Ulbrich, R., Mewes, D., 1994. Vertical, upward gas–liquid two-phase flow across a tube bundle. Int. J. Multiphase Flow 20, 249–272.